



EXPERIMENTAL AND NUMERICAL INVESTIGATION OF FIXED CONNECTIONS OF RC CLADDING WALLS TO PRECAST BUILDINGS

Ioannis N. PSYCHARIS¹, Ioannis KALYVIOTIS² and Harris P. Mouzakis³

ABSTRACT

Recent earthquakes have dramatically shown the importance of cladding connections on the seismic response of precast buildings. In the present work, an experimental and numerical investigation on the monotonic and cyclic behaviour of ‘fixed’ connections, referred also as “integrated” connections, is reported. In this case, simplified structural calculations show that the seismic forces induced to the connections of the panels can be quite large for typical structures. An extensive experimental program has been performed at the Laboratory for Earthquake Engineering of the National Technical University of Athens, Greece, within the framework of the FP7 European project SAFECLADDING, for the investigation of the behaviour of integrated connections. The experimental campaign is still ongoing, thus only results concerning ‘rebar’ type of connections, i.e. connections materialised with vertical reinforcement bars, are reported here. The results show that such connections have considerable ductility capacity; however, significant opening and slipping was observed at the joints for large displacements, making questionable whether such connections can be designed for ductile response. A numerical model was also constructed and calibrated against the experimental results, which can be used for non-linear analyses of buildings with integrated cladding walls.

INTRODUCTION

In common design practice of precast structures, cladding panels are not designed to contribute to the structure’s lateral stiffness but are connected to the structure with fastening devices dimensioned to bear the panels’ self-weight, wind loads and seismic loads corresponding to the panels’ mass only. However, the behaviour of cladding wall systems in recent strong earthquakes (e.g. L’Aquila, 2009 and Grenada, 2010 in Italy) dramatically showed that cladding panels become an integral part of the structure’s lateral resisting system during intense shaking, resulting to severe damage to the connections which can even lead to fall of the panels.

New innovative panel-to-structure connections and novel design approaches for a correct conception and dimensioning of the fastening system to guarantee good seismic performance of the structure are investigated within the FP7 project: “SAFECLADDING: Improved fastening systems of cladding wall panels of precast buildings in seismic zones”. Part of this investigation concerns fixed panel connections, also referred as “integrated” connections, which are designed to restrict large relative displacements and capable to sustain the large forces developed.

In the integrated systems, the panel connections are based on a hyperstatic arrangement of the fixed supports of each panel and, thus, the panels participate in the earthquake load bearing system.

¹ Professor, National Technical University, Athens, Greece, ipsych@central.ntua.gr

² Ph.D. Candidate, National Technical University, Athens, Greece, ikalyvio@central.ntua.gr

³ Ass. Professor, National Technical University, Athens, Greece, harrismo@central.ntua.gr

Several arrangements can be used to this end, such as vertical panels connected to the beams (Fig. 1a) or horizontal panels connected to the columns (Fig. 1b). In both cases, connections at all four corners of each panel are provided and the panel elements act as beams clamped at both ends. Configurations with fewer connections (e.g. three connections, one at one end and two at the other) are also possible; however, one must have in mind that the reduction of the number of the connections leads to twice larger forces induced to the connectors.

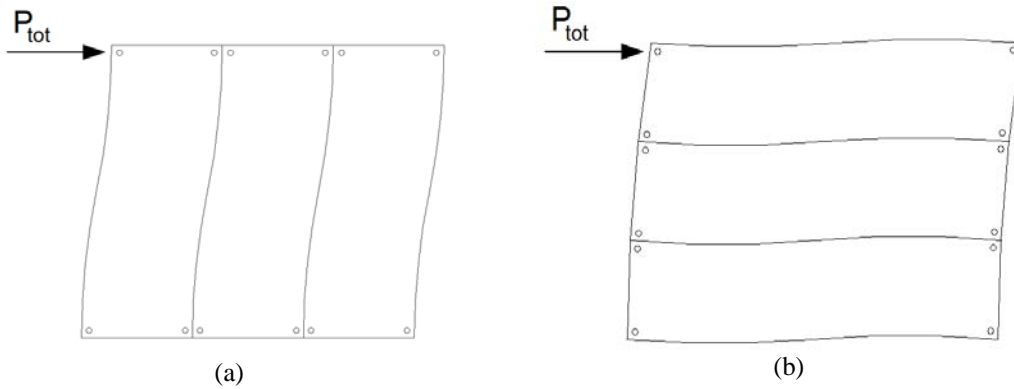


Figure 1. Typical deformation of panels with four fixed connections: (a) vertical panels connected to the beams; (b) horizontal panels connected to the columns.

In case of horizontal panels, it is recognized that the fixed connections to the columns affect significantly the deformation of the columns during earthquakes. Moreover, any damage during strong seismic excitation may have disastrous consequences to the overall strength of the columns and the stability of the whole building. Additionally, their construction is problematic. Therefore, horizontal panel arrangement in integrated systems is not recommended. For this reason, the experimental campaign was limited to vertical panels only.

In this paper, the first experimental results, which concern the ‘rebar’ type of integrated connections (described in the ensuing) are reported. For such connections, a numerical model was also constructed, which was calibrated and validated against the experimental data. Application of this model allows the derivation of the constitutive law that governs the non-linear response of panel-to-beam connections of any dimensions, which can be used in non-linear analyses of precast structures with fixed cladding wall panels.

ESTIMATION OF THE CONNECTION FORCES

Simple structural considerations, based on the assumption of panels fully fixed at all four corners, can give a good estimation of the forces that develop at integrated connections during the seismic action. This simplified analysis is presented in the following for vertical panels connected to the beams. It is mentioned that these results have been verified by more rigorous finite element analyses.

Let us consider a symmetric building on which the cladding wall panels are placed at the two external sides along the direction of the seismic action. Taking into account the large stiffness of the panels compared with the stiffness of the precast frame, it can be assumed, approximately, that the total base shear due to the earthquake load is undertaken solely by the panels.

Let n be the number of the panels at each side of the building (vertical panels) and that each panel is fixed to the top and the bottom beam by two connectors at each side. Then, the horizontal force, P_h , induced to each connection is (Fig. 2):

$$P_h \cong \frac{P_b}{4n} \quad (1)$$

where P_b is the total earthquake load (base shear).

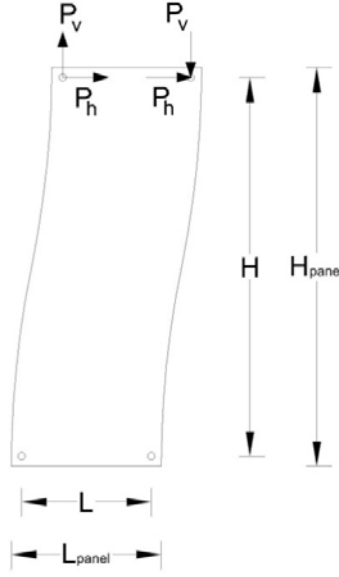


Figure 2. Distribution of forces at the connections of fixed vertical panels.

For fully clamped conditions, the vertical forces developed at the connections are:

$$P_v = P_h \frac{H}{L} = P_b \frac{H}{4nL} \quad (2)$$

In the above equation, H is the vertical distance between the connections of the panel and $L = C_1 \cdot L_{panel}$ is the corresponding horizontal distance (Fig.2). These distances are smaller than the actual dimensions of the panel due to the insertion of the connections from the panel's edges.

The total force developed in one connection is:

$$P_c = \sqrt{P_h^2 + P_v^2} \quad (3)$$

Taking into account that the total length L_{tot} of the building's sides on which the panels are placed is not necessarily fully covered with panels, i.e. $n \cdot L_{panel} = C_2 \cdot L_{tot}$, C_2 being the portion of the façades covered with panels in the direction under consideration, one can write: $nL = C_1 C_2 L_{tot}$. Then, the force at each connection, normalized with respect to the total seismic load, can be written as:

$$\frac{P_c}{P_b} = \frac{1}{4} \sqrt{\frac{1}{n^2} + \left(\frac{H}{C_1 C_2 L_{tot}} \right)^2} \quad (4)$$

Note that the second term under the square root is independent of the number of panels and depends only on the coverage, C_2 , of the sides with panels. For typical dimensions of industrial and residential buildings and for values of n larger than about 4, the term $1/n^2$, which corresponds to the horizontal component of P_c , can be neglected in Eq. (4). Therefore, the force induced to each connection is applied mainly in the vertical direction and can be approximated by:

$$P_c \cong P_v = P_b \cdot \frac{H}{4C_1 C_2 L_{tot}} \quad (5)$$

Eq. (5) implies that the force induced to each connection is practically independent of the width of the panels, which means that the connection forces cannot be reduced by using more panels of smaller length or less panels of larger length. However, it greatly depends on the coverage of the

façades with panels, C_2 , and increases significantly in case of large openings, when C_2 is considerably less than unity. Also, the force induced to each connection is linearly increasing with the vertical distance H of the connections, i.e., with the height of the storey.

As an example, let us consider a 3-storey building with plan dimensions $10.00 \text{ m} \times 20.00 \text{ m}$ and storey height 3.50 m , covered with panels of dimensions: $L_{panel} = 2.00 \text{ m}$, $H_{panel} = 3.00 \text{ m}$, $L = 1.60 \text{ m}$ (i.e. $C_1 = 0.80$) and $H = 2.70 \text{ m}$. Due to openings, it is assumed that only a portion of each façade is covered with panels, specifically it is considered that $n = 3$ in the short direction ($C_2 = 0.60$) and $n = 7$ in the long direction ($C_2 = 0.70$). Taking the floor weight equal to $w = 10.00 \text{ kN/m}^2$ for all stories, and assuming that the ground acceleration is $a_g = 0.24 \text{ g}$ and the soil is of category B ($S = 1.20$ according to Eurocode 8), and that the spectral amplification is $Se/(S \cdot a_g) = 2.5$ (horizontal branch of the elastic design spectrum), the total base shear for $q = 1$ (elastic behaviour) is $P_b = 4320 \text{ kN}$. Then, Eq. (5) leads to the following connection forces for the panels of the ground floor: $P_c = 607.5 \text{ kN}$ in the short direction and $P_c = 260.4 \text{ kN}$ in the long direction.

It is noted that the above values are for elastic design ($q = 1$). If a larger value of the behaviour factor q is adopted, these values are reduced accordingly. In any case, this simplified analysis shows that fixed panel connections need to be designed for considerably large forces, thus, special research is needed for the investigation of the behaviour of such connections.

EXPERIMENTAL PROGRAMME AND SETUP

The experimental campaign concerns a series of tests on panels connected to beams with fixed connections. Three types of connections are examined, namely:

- ‘Rebar’ connections (Fig. 3a) made of reinforcement bars which protrude from the beam into the panel or vice versa;
- ‘Steel plate’ connections (Fig. 3b) in which the connection of the panel to the beam is achieved using a steel plate;
- Industrially manufactured connecting mechanisms, as the wall shoes shown in Fig. 3c.

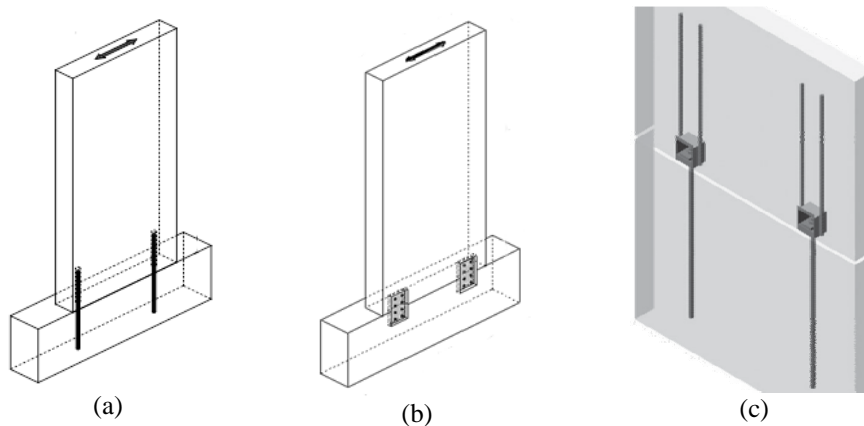


Figure 3. Connection types considered in the experiments: (a) ‘rebar’ connections; (b) ‘steel plate’ connections; (c) industrial wall shoes.

The experimental programme is still ongoing and only results concerning tests on ‘rebar’ connections are reported herein.

The specimens consisted of a panel wall connected to a bottom beam fastened to the strong floor of the Laboratory. The force was applied at the free top of the wall using a specially designed steel mechanism which was fastened to the panel through six bolts in order to obtain a uniform distribution of the load. This configuration represents one half of a prototype with double the height of panel model, fully connected at its four corners. The experimental setup is shown in Fig. 4.

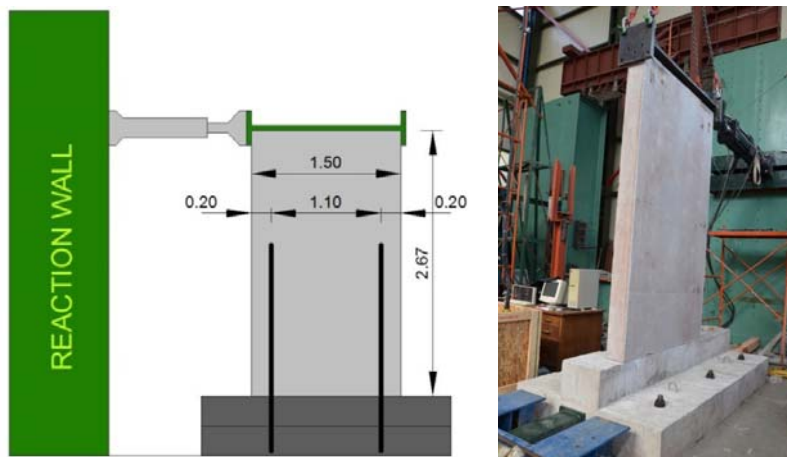


Figure 4. Experimental setup and photo of the specimens tested.

The specimens were made in physical scale. The panel walls had dimensions: 2.67 m in height, 1.50 m in length and were 0.18 m thick, while the beams were of cross section 0.40 m \times 0.60 m. The length of the wall models (1.50 m) is considered small for typical panels used in industrial buildings, but it was chosen in order to reduce the size of the specimens as much as possible, taking under consideration that the length does not affect the response of the connections, which was the main objective of the experimental campaign. Additionally, the vertical force induced to the connections for a specific value of the horizontal force applied at the top of the wall increases as the length of the panel decreases, thus, ‘short’ walls allowed to test stronger connections without exceeding the limits of the hydraulic actuator. For this reason, a relatively small length was chosen, which, however, was long enough to guarantee that the two connections were sufficiently apart from each other to prevent interaction effects between them.

For the ‘rebar’ connections, vertical reinforcement bars of two diameters, namely 1 \varnothing 20 and 1 \varnothing 25 at each connection, were tested. The bars protruded from the panels into the beams or vice versa and the gap between the bars and the waiting ducts was filled either with epoxy resin or with high strength grout. It is recognised that this type of connection has mounting difficulties, rising from the protruding bars.

The specimens were designed for concrete grade C30/37 and steel grade B500C in accordance with EN 1992-1-1 and EN 1998-1, following the results of a finite element analysis using SAP2000 (the numerical model is described in a subsequent section). Indicative reinforcement drawings are shown in Fig. 5. More details can be found in Psycharis *et al.* (2013).

Five tests were performed, three monotonic and two cyclic, as shown in Table 1. In monotonic tests, reverse loading was applied after failure of the connection in tension. However, it was not always possible to break the second connection too, because full contact with the beam in the compression zone could not be re-established, due to the permanent plastic deformation of the broken rebar. This issue is further discussed later, when the experimental results are presented.

Table 1. Experimental Programme for ‘rebar’ connections.

No.	Test	Connection			Nominal strength* (kN)	Loading
		Type	Rebars	Connecting material		
1	A1D20M-R1	Rebars	1 \varnothing 20	Epoxy resin - 1	137	Monotonic
2	A1D20C-R1	Rebars	1 \varnothing 20	Epoxy resin - 1	137	Cyclic
3	A1D25M-R2	Rebars	1 \varnothing 25	Epoxy resin - 2	213	Monotonic
4	A1D25M-G	Rebars	1 \varnothing 25	Grout	213	Monotonic
5	A1D25C-G	Rebars	1 \varnothing 25	Grout	213	Cyclic

* The nominal strength corresponds to the axial resistance of B500C rebars for $\gamma_s = 1.15$.

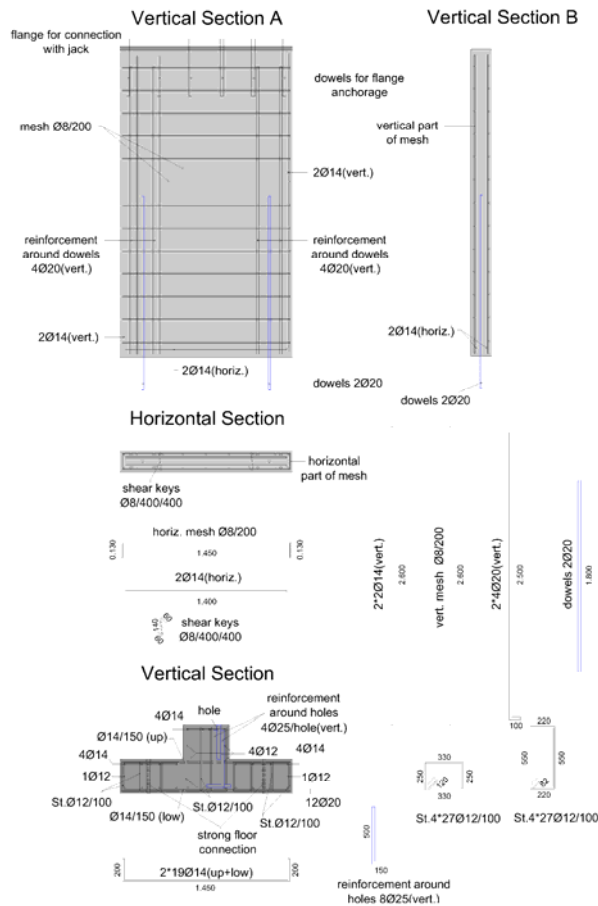


Figure 5. Reinforcement details of specimens A1D20M-R1 and A1D20C-R1

For cyclic loading, the applied loading history (Fig. 6) was based on the protocol proposed in FEMA 461 (2007). The loading history consisted of repeated cycles of step-wise increasing deformation amplitudes by 40%. The number of steps with different amplitudes was equal to ten, with two cycles included in each step. The final target value Δ_m was set equal to the maximum displacement achieved for monotonic loading, while the initial target value Δ_0 was determined so that Δ_m is reached at the 10th amplitude increment, i.e. $\Delta_0 = \Delta_m/1.4^9$.

Concerning the instrumentation, the displacements at critical positions and the deformation of the connecting bars and the concrete of the panel in the vicinity of the joint were measured during the experiments. Specifically, horizontal and vertical displacements were measured at 10 points using displacement transducers, while 16 strain gauges were used to measure the deformation of the connection rebars and the concrete. In most cases, displacements and strains were measured at both sides of the panel.

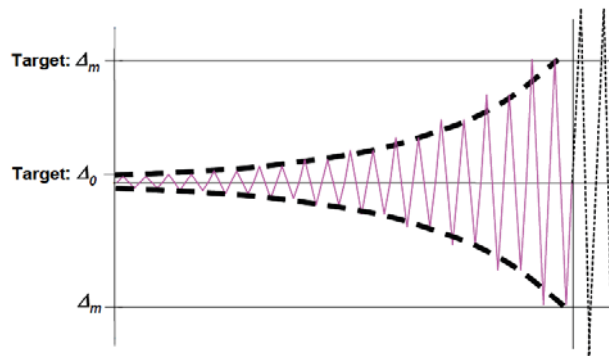


Figure 6. Sketch of loading history applied in cyclic tests.

EXPERIMENTAL RESULTS

The horizontal force versus the top displacement of the specimens with connections made of 1Ø20 rebars under monotonic and cyclic loading is shown in Fig.7. In both tests, the rebars were protruding, about 0.30 m, from the panel into the beam and the bond with the concrete was achieved using epoxy resins.

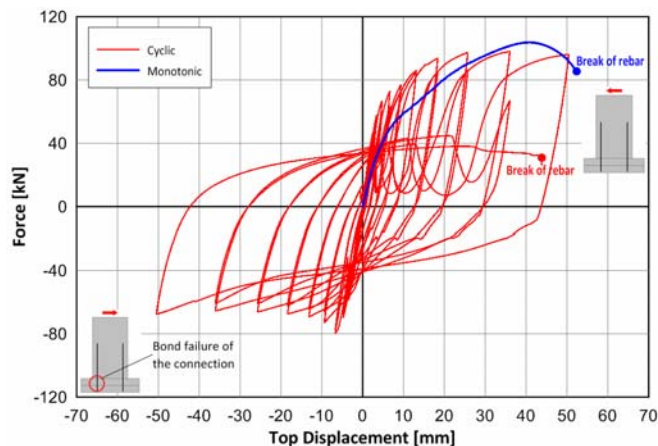


Figure 7. Horizontal force vs. top displacement for connections made of 1Ø20 rebars under cyclic and monotonic loading.

For monotonic loading, the maximum top displacement achieved before the breakage of the rebar under tension was about 50 mm and the maximum horizontal force was about 100 kN. The response under cyclic loading was, in general, following the capacity curve for monotonic loading in what regards both the maximum attained displacement and the resistance, but it showed larger elastic stiffness. During the cyclic experiment, bond failure happened to the rebar of one of the connections (the one that was under tension for negative displacements, see Fig.7) resulting to non-symmetric response. Due to the slippage of the rebar, which started at about $d_{top} = -7$ mm and $F_{hor} = 80$ kN, the response was characterized by a softening behaviour for negative displacements (bottom left quarter of diagram in Fig.7) and a sudden loss of strength for positive displacements (top right quarter of diagram in Fig.7). However, when all the slippage that had occurred during the previous cycle was absorbed, the strength was regained and the force started increasing again.

Apart of the aforementioned bond failure of one of the connections, the cyclic response was characterized by significant pinching, which is attributed to the elongation of the rebars due to the accumulation of plastic deformation. Due to this permanent elongation of the rebars, a gradually increasing opening of the joint between panel and beam occurred, which is shown in Fig. 8a for monotonic and cyclic loading. In the latter case, the panel-to-beam contact could not be re-established for small top displacements (i.e. close to the initial position) and the horizontal force was undertaken solely by the dowel action of the rebars, without any participation of the friction mechanism, resulting in large displacement at the base of the panel; as can be seen in Fig. 8b, there was an obvious slip of the panel with respect to the beam, which initially increased almost linearly with the top displacement. For larger displacements, however, this slip stopped, due to the rotation of the panel and the re-establishment of the panel-to-beam contact and the friction mechanism.

Anchorage length of 0.30 m combined with the use of resins was also applied to the specimen with connections made of 1Ø25 rebars that was tested under monotonic loading. Again, this length was proven insufficient and bond failure occurred to the rebar quite early in the test. For this reason, the test was repeated increasing significantly the anchorage length of the rebars to 1.30 m (the bars were now protruding from the beam into the panel) and using high-strength, non-shrinking grout instead of resins. The horizontal force – top displacement relation for monotonic loading is depicted in Fig. 9 (red line). In this figure, the corresponding curve for the specimen with 1Ø20 connections (blue line) is also shown for comparison. It is seen that the connections made of 1Ø25 had almost 50% larger resistance, a value close to the increase in the cross section of the rebars of the connections, and significantly larger displacement capacity (65% larger).

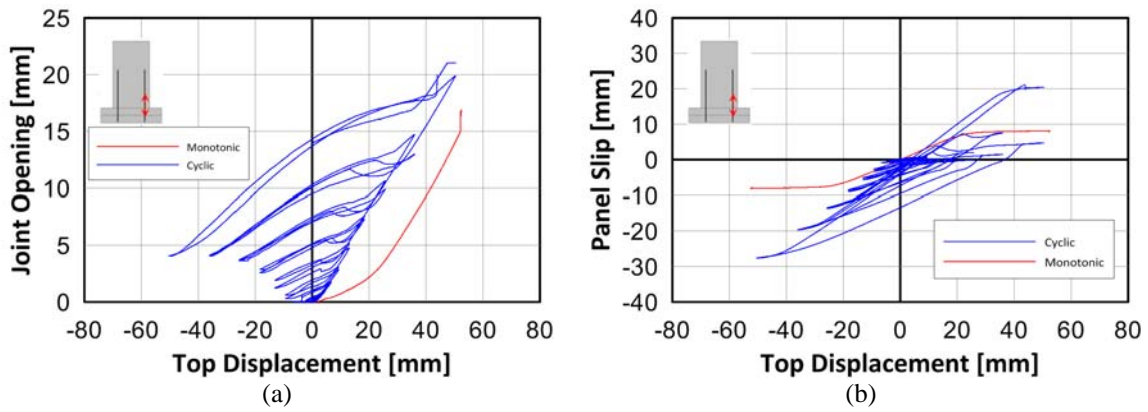


Figure 8. Connections made of 1Ø20 rebars: (a) joint opening vs. top displacement; (b) horizontal slip vs. top displacement.

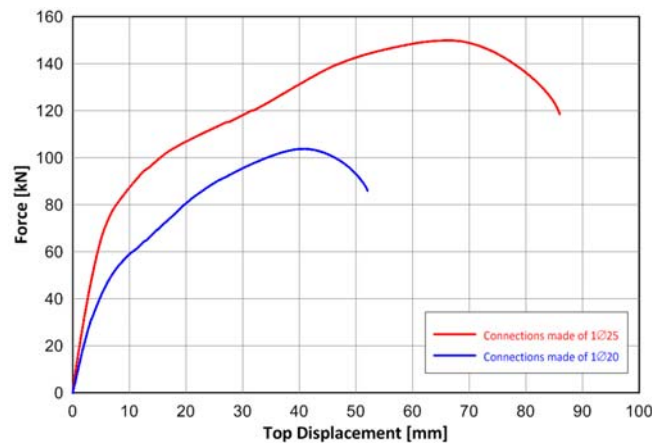


Figure 9. Horizontal force vs. top displacement for monotonic loading of specimens with connections made of 1Ø25 rebars (red line) and 1Ø20 rebars (blue line).

The cyclic test for connections made of 1Ø25 rebars was also performed to a specimen with extended anchorage length (1.30 m) and using grout. In Fig.10, the cyclic behaviour is compared with the monotonic one. As in the case of connections made of 1Ø20 rebars, it is seen that the envelope of the cyclic response followed, in general, the monotonic one; however, the connection bar broke in significantly smaller displacement than for monotonic loading. Again, the cyclic response showed significant pinching for large displacements which, as already explained, was accompanied with gradually increasing joint opening and horizontal slip of the panel.

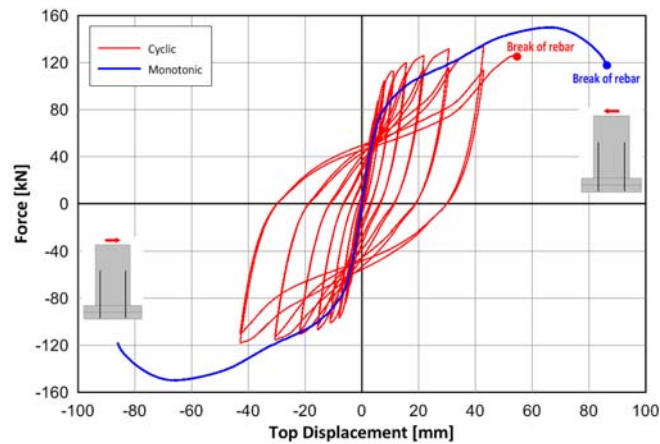


Figure 10. Horizontal force vs. top displacement for connections made of 1Ø25 rebars under cyclic and monotonic loading.

Table 2. Summary of the experimental results

	A1D20M-R1	A1D20C-R1	A1D25M-R2	A1D25M-G	A1D25C-G
Yield strength ⁽¹⁾ [kN]:	56	67	-	87	105
Maximum strength [kN]:	104	98	-	150	134
“Yield” displacement ⁽¹⁾ d_y [mm]:	9	5	-	10	8
Displacement at maximum strength d_{fmax} [mm]:	40	36	-	66	53
Ultimate displacement $d_{u,tot}$ [mm]:	52	50	-	86	43
Ductility ⁽²⁾ of initial loading:	4.4	7.2	-	6.6	5.4
Ductility ⁽²⁾ of reverse loading:	-	-	-	-	7.5
Panel’s bottom slip [mm]:	8	28	-	10	21
Maximum joint opening ⁽³⁾ [mm]:	17	20	-	30	11

⁽¹⁾ The yield point corresponds to the significant change in stiffness in the curve and does not necessarily refer to the yielding of the rebar.

⁽²⁾ The ductility is calculated as d_{fmax}/d_y .

⁽³⁾ The joint opening is measured at the position of the bars.

The results of all experiments on ‘rebar’ connections are summarized in Table.2.

Concerning the damage, mainly spalling of the concrete was observed at the faces of the panel and the beam around the connections (Fig.11), which, however, occurred for considerably large displacements.

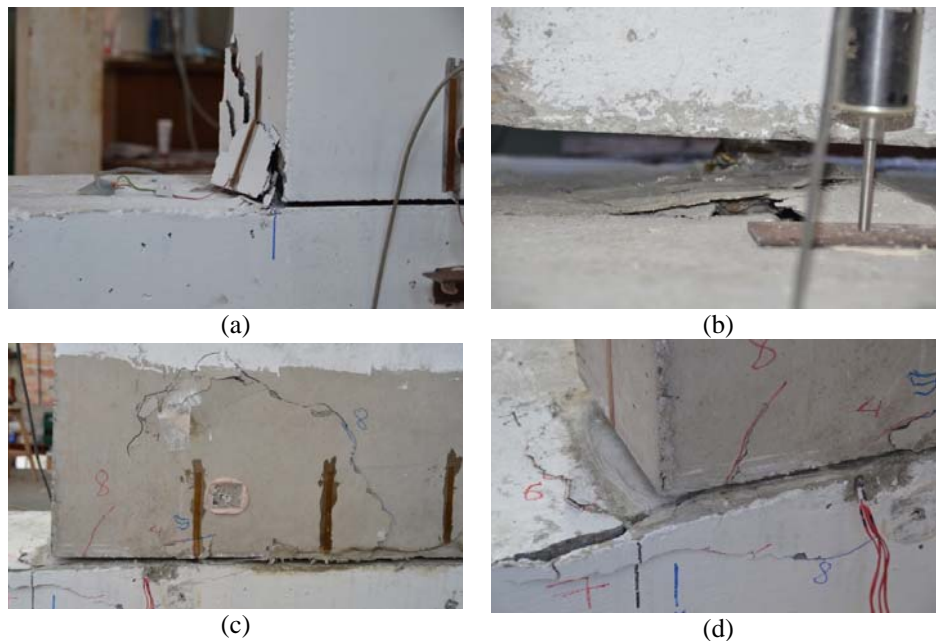


Figure 11. Observed damage at the end of the tests: (a) spalling of the concrete at the side face of the panel; (b) spalling of the concrete at the top of the beam around the rebar; (c) spalling of the concrete of the panel around the connection; (d) spalling of the concrete of the beam close to the connection.

NUMERICAL MODEL

The experimental tests were reproduced numerically using typical modelling of reinforced concrete structures (fib Bulletin 45). The numerical model consisted of the panel wall connected to the beam at its bottom (Fig. 12). Both the panel and the beam were modelled with shell elements, while the connections’ rebars were modelled with beam elements. The joint between the panel and the beam was modelled with tensionless springs (gap elements).

A special arrangement had to be applied in order to capture accurately the behaviour of the rebars. Thus, the nodes of the rebars were not connected directly to the corresponding nodes of the shell elements (panel and beam) but through nonlinear springs, in order to model realistically the bonding between the rebars and the surrounding concrete. The behaviour of these springs was elastic –

perfectly plastic, allowing the local loss of bond when the corresponding bond strength was exceeded. In order to capture accurately the spatial distribution of the bond-yielding, a quite dense mesh was used around the rebars (the node distance was 20 mm). More details on the numerical model can be found in Kalyniotis (2013).

Representative numerical results are shown in Fig. 13: in Fig. 13a, the deformation at large top displacement (final step of the analysis) is presented, while in Fig. 13b, the corresponding distribution of the axial forces along the rebar is depicted.

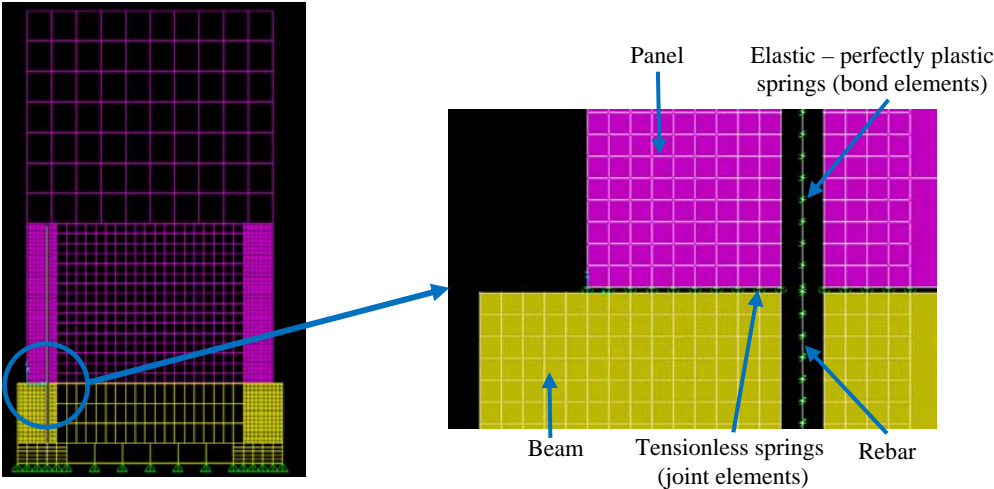


Figure 12. Model used for the analyses of the inelastic behaviour of panel – beam connections.

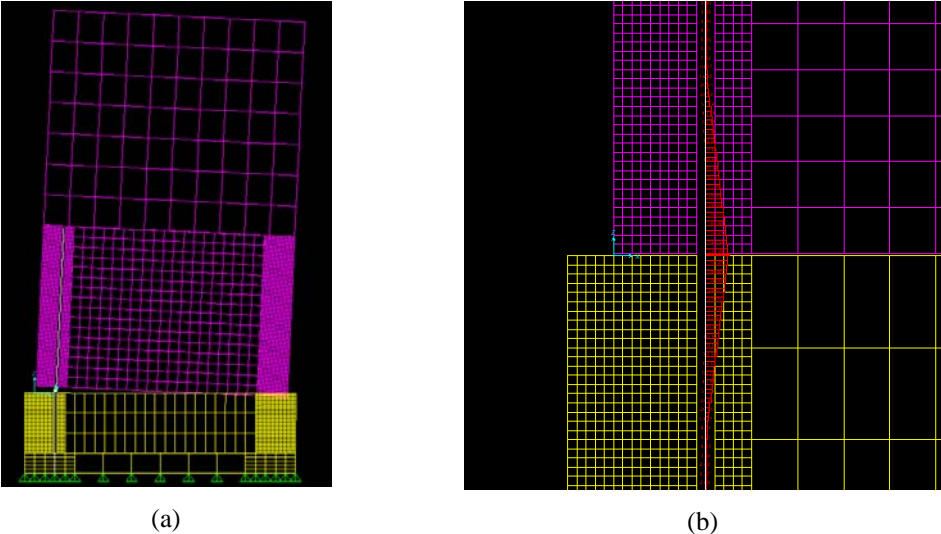


Figure 13. Representative numerical results: (a) deformed shape; (b) axial force induced to the rebar at the final step of the analysis.

As expected, the nonlinear ‘bond’ springs governed the response of the system and, therefore, the proper definition of their properties is of vital importance. For this reason, the model was calibrated against the results of the experiments, using the backbone curve of the corresponding cyclic response. In Figures 14 and 15, the curves showing the relation between the horizontal force and the top displacement of the panel, obtained from the numerical analyses for connections made of 1Ø20 and 1Ø25 rebars (red lines), are compared with the experimental results (cyclic and monotonic). It is seen that the numerical results capture accurately the initial (elastic) stiffness and the hardening slope after yield, but overestimate, somehow, the yield force. In general, however, the comparison of the numerical results with the experimental data shows that the numerical model could capture quite accurately the overall behaviour of the panel-to-beam connection and the distribution of the forces along the connection bars.

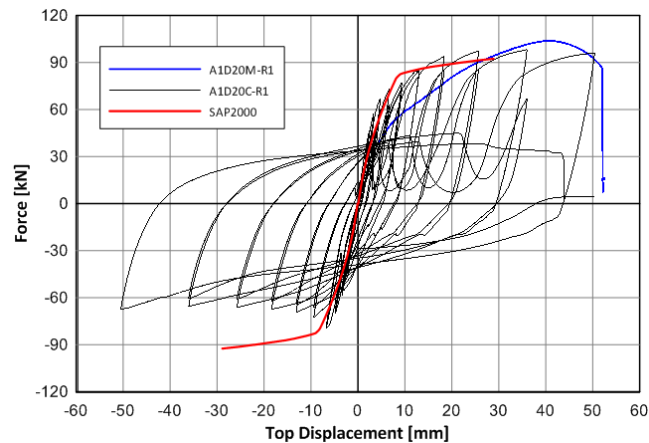


Figure 14. Connections made of 1Ø20 rebars: comparison of numerical results with experimental data.

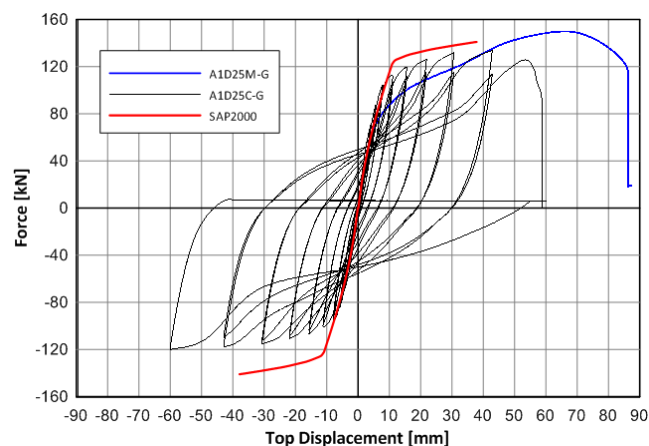


Figure 15. Connections made of 1Ø25 rebars: comparison of numerical results with experimental data.

The verification of the numerical model allows its application for the development of capacity curves of ‘rebar’ connections of any dimensions that can be used in numerical models of precast buildings with integrated panel walls for nonlinear time-history analyses.

CONCLUSIONS

In this paper, the first experimental results on integrated panels connections of the ‘rebar’ type, performed in the framework of the FP7 project SAFECLADDING, are presented. The conclusions drawn from the performed tests and the analytical and numerical investigation of the response of the connections can be summarized as follows:

- The major component of the force induced to each connection is in the vertical direction. For this reason, ‘rebar’ connections provide, in principle, an effective mechanism for the connection of the panel with the beam, since the rebars are stressed mainly in tension.
- The force induced to each connection increases with the vertical distance of the connections along the height of the panel, i.e., with the height of the storey, but it is practically independent of the length of the panels. Therefore, the connection forces cannot be reduced by using more panels of smaller length or less panels of larger length. However, the connection forces greatly depend on the ‘coverage’ of the façades with panels.
- The ultimate resistance of the connections is proportional to the cross section of the rebars.
- Sufficient anchorage length of the rebars in conjunction with the use of proper bonding materials should be provided in order to guarantee that no slippage of the rebars will occur.

- The cyclic response is characterized by pinching of the hysteretic loops for large displacements. Pinching is caused by the accumulation of plastic deformation in the rebars (permanent elongation), which causes permanent opening of the joint preventing full contact of the panel with the beam.
- The attained ductility of the connections under cyclic loading was more than five. However, it is questionable whether the connections should be design for ductile response due to the aforementioned pinching phenomena and the permanent separation of the panel from the beam for large displacements.

ACKNOWLEDGEMENTS

The research presented herein was conducted within the project “SAFECLADDING: Improved fastening systems of cladding wall panels of precast buildings in seismic zones”, which was financed by the European Commission in the framework of the Seventh Framework Programme (FP7) under Grant Agreement number 314122. The second author wants to thank the Onassis Foundation for the financial support of his postgraduate studies at NTUA through Scholarship number GZI015. Special thanks are due to Dr Lucia Karapitta for her help in the execution of the experiments and the processing of the data and to the concrete company Interbeton S.A. for supplying the concrete for the construction of the specimens.

REFERENCES

- European Committee for Standardization (CEN) (2004) Design of concrete structures – Part 1-1: General rules and rules for buildings, EN 1992-1-1
- European Committee for Standardization (CEN) (2004) Design of structures for earthquake resistance – Part 1: General rules, seismic actions and rules for buildings, EN 1998-2
- Federal Emergency Management Agency (FEMA) (2007) Interim Testing Protocols for Determining the Seismic Performance Characteristics of Structural and Nonstructural Components, Report 461
- International Federation for Structural Concrete (fib) Practitioners’ guide to finite element modelling of reinforced concrete structures, Fib Bulletin 45, State-of-the art report prepared by Task Group 4.4
- Kalyviotis I. (2013) Analytical and experimental investigation of fixed connections of RC cladding walls to precast buildings, MSc. Thesis, National Technical University, Athens, Greece
- Psycharis I.N., Mouzakis H.P., Kalyviotis I., et al. (2013) Report and card files on tests performed on connections for integrated systems, SAFECLADDING: Improved fastening systems of cladding wall panels of precast buildings in seismic zones, Deliverable 3.2, FP7 Project: GA No. 314122